

Addressing Practical Challenges of Low Friction Coefficient Measurements

D. L. Burris · W. G. Sawyer

Received: 26 December 2008 / Accepted: 25 March 2009 / Published online: 10 April 2009
© Springer Science+Business Media, LLC 2009

Abstract A friction coefficient is defined as the ratio of the friction force to the applied normal force. Despite the disarming simplicity of its calculation, there are practical challenges that make low values of friction coefficient difficult to accurately quantify. The connections of imperfect parts in friction measurement devices (called tribometers) produce small misalignments between the transducer and counterface axes. According to Schmitz et al. (J Tribol Trans ASME 127:673–678, 2005), “...the measurement of friction coefficient is extremely sensitive to misalignments” and “for materials with friction coefficients below 0.05 the alignment becomes hopelessly difficult if the goal is to have uncertainties below 1%.” This method article reviews the challenges of low friction measurements and presents a robust reversal technique that eliminates misalignment bias. Experiments with controlled misalignment angles demonstrate the bias sensitivity and validate its elimination using a low uncertainty tribometer in conjunction with the described reversal technique.

Keywords Friction coefficient · Tribometer · Uncertainty · Measurement · Statistics

1 Friction Coefficient Measurements

Friction force measurements provide insights into the fundamental interactions of surfaces and an empirical basis for machine design. A friction coefficient is defined, as shown in Eq. 1, as the ratio of the force resisting motion (friction force, F_f) to the applied normal force (F_n).

$$\mu = \frac{F_f}{F_n} \quad (1)$$

In general, friction coefficients range from about 0.2 to 1 for typical material pairs under standard conditions. Values much greater than 1 are not uncommon in vacuum and a number of modern materials have exhibited ‘super lubricity’ with friction coefficients well under $\mu = 0.01$.

Values of friction coefficient are often reported for common material pairs in handbooks to guide preliminary designs. Engineers mistakenly use these values as they would use tabulated values of yield stress. In reality, material pairs do not have singular characteristic values of friction coefficient. The friction coefficient is extremely sensitive to the lubrication, environment, and contact conditions, and under nominally constant conditions, it can exhibit large time dependent variations over a range of time-scales.

Scientists often calculate statistics from measurements to provide an indication of the population mean and variance, both of which are valuable to design engineers. In addition to inherent variations in the interfacial friction coefficient, the measured value *always* deviates from the true value of the measured quantity. The measurement uncertainty describes the “dispersion of values that could reasonably be attributed to the measurand” [2]. Measurement uncertainties are critical to scientific studies because they provide the reader with an indication of the quality of

D. L. Burris (✉)
Department of Mechanical Engineering, University of Delaware,
Newark, DE 19716, USA
e-mail: dlburris@udel.edu

W. G. Sawyer
Department of Mechanical and Aerospace Engineering,
University of Florida, Gainesville, FL, USA

the measurements; despite their importance, discussions of measurement uncertainties are almost completely absent from the tribology literature. Schmitz et al. [1] conducted a detailed uncertainty analysis of a friction measurement and found that transducer misalignment generally dominates the friction coefficient uncertainty.

2 Effects of Transducer Misalignment on Friction Coefficient Bias

A calculation of friction coefficient requires normal force and friction force measurements. In practice, however, neither can be directly measured. A typical experimental configuration is illustrated in Fig. 1, where the friction and normal forces are reacted by a force transducer. Ideally, the counterface surface defines the orientation of the transducer, and the reaction forces are equal to the interfacial forces. In reality, the transducer and counterface are separated by an assembly of imperfect parts which results in a misalignment angle between the vertical (Y) axis of the transducer and the counterface normal (to which μ is referred). The measured friction coefficient, μ' , is defined by the ratio of the transducer forces; $\mu' = \frac{F_X}{F_Y}$. For simplicity, the X and Y axes are assumed orthogonal (assembly misalignment dominates the squareness error of any single component). The entire transducer in Fig. 1 is displaced by a single misalignment angle, α , from the counterface normal. The transducer forces and the measured friction coefficient, μ' , are given by Eqs. 2, 3, and 4 using a condition of static equilibrium and the definition of the interfacial friction coefficient, $\mu = \frac{F_f}{F_n}$.

$$F_X = \mu F_n \cos(\alpha) - F_n \sin(\alpha) \quad (2)$$

$$F_Y = F_n \cos(\alpha) + \mu F_n \sin(\alpha) \quad (3)$$

$$\mu' = \frac{F_X}{F_Y} = \frac{\mu F_n \cos(\alpha) - F_n \sin(\alpha)}{F_n \cos(\alpha) + \mu F_n \sin(\alpha)} = \frac{\mu \cos(\alpha) - \sin(\alpha)}{\cos(\alpha) + \mu \sin(\alpha)} \quad (4)$$

The measured friction coefficient is a function of both the interfacial friction coefficient, μ , and the misalignment angle, α . The measured friction coefficient and the ratio of the measured friction coefficient to the interfacial friction coefficient are plotted versus angular misalignment in Fig. 2 for $\mu = 0.1$, 0.01, and 0.001. The measured friction coefficients decrease with angle at the same rate, but the measurement error is much more sensitive to misalignment at lower values of friction coefficient. According to Schmitz et al. [1], "...the measurement of friction coefficient is extremely sensitive to angular misalignments between the loading axis and the counterface" and "for materials with friction coefficients below 0.05 the alignment becomes hopelessly difficult if the goal is to have uncertainties below 1%."

Schmitz et al. [1], used static force measurements to calculate an angular misalignment of approximately 2.5°; for $\mu = 0.1$ and $\mu = 0.01$, the corresponding errors are 40% and 400%, respectively. The authors used this measurement with Eq. 4 to solve for the interfacial friction coefficient. Although the bias can be corrected using this method, the angular measurements are difficult to make and are themselves subject to significant uncertainties. A reversal technique has been developed here to address these challenges. As shown in the following discussion, this method completely eliminates misalignment sensitivity without requiring knowledge of the misalignment angle.

Fig. 1 Schematic representation of a typical friction coefficient measurement; **a** forward sliding, **b** reverse sliding. Assembly of parts with realistic manufacturing tolerances results in an angular misalignment of the transducer with respect to the counterface. As a result, the forces on the transducer axes are not identical to the friction and normal forces. The friction coefficient measurement, μ' , is biased from the interfacial friction coefficient, μ

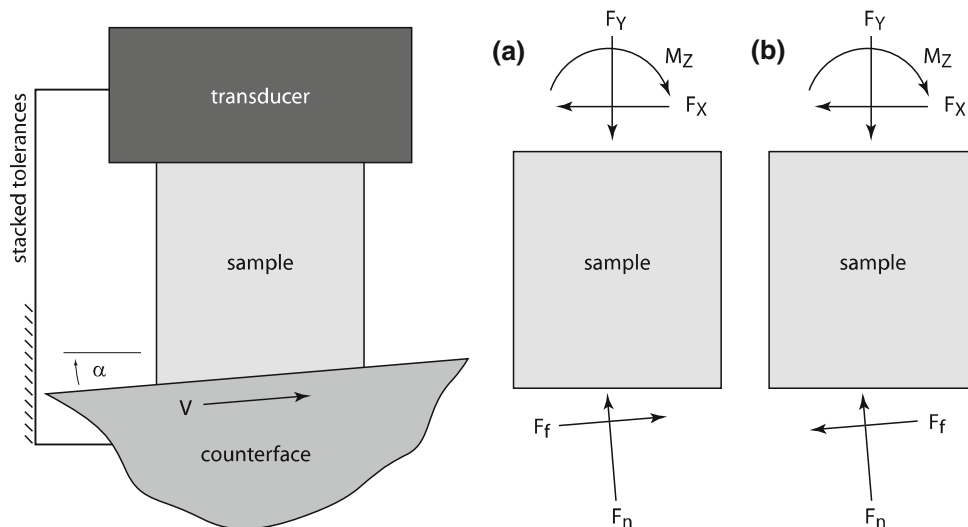
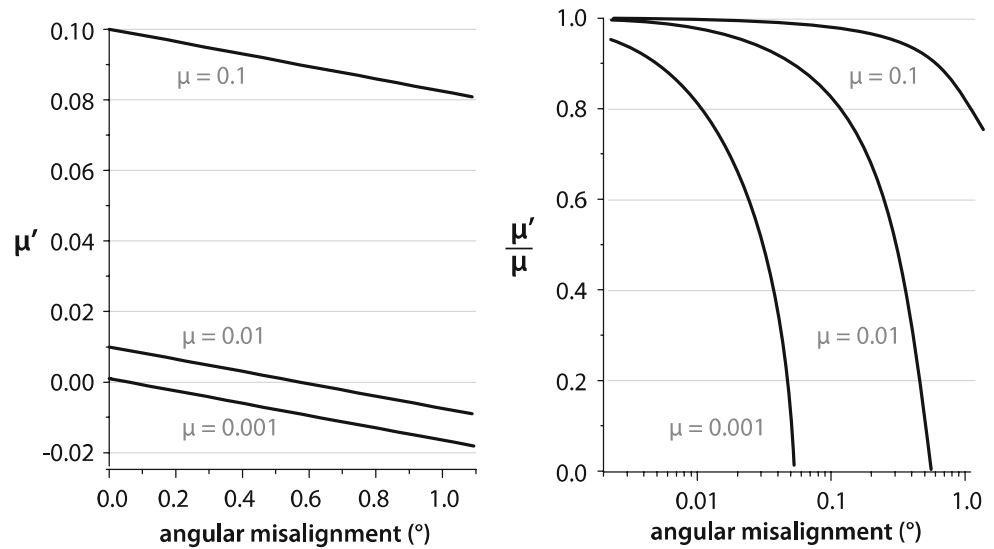


Fig. 2 Left: the forward friction coefficient, μ'_f , plotted versus the angular misalignment for different values of the interfacial friction coefficients, μ . Right: the measured friction coefficient normalized to the interfacial friction coefficient for different values of μ . In all three cases, significant errors result from slight misalignment angles. Measurements of ‘superlow’ values of friction coefficient (<0.01) are especially difficult to defend using standard methods



3 Reducing Misalignment Sensitivity

If the sliding direction is reversed (as is naturally the case in reciprocating experiments), the friction force is also reversed as shown in Fig. 1b. The measured forces and friction coefficient in the reverse direction are given by Eqs. 5, 6, and 7.

$$F_{Xr} = -\mu F_n \cos(\alpha) - F_n \sin(\alpha) \tag{5}$$

$$F_{Yr} = F_n \cos(\alpha) - \mu F_n \sin(\alpha) \tag{6}$$

$$\mu'_r = \frac{F_{Xr}}{F_{Yr}} = \frac{-\mu F_n \cos(\alpha) - F_n \sin(\alpha)}{F_n \cos(\alpha) - \mu F_n \sin(\alpha)} = \frac{-\mu \cos(\alpha) - \sin(\alpha)}{\cos(\alpha) - \mu \sin(\alpha)} \tag{7}$$

For subsequent discussions, f denotes forward and r denotes reverse directions. The fortuitous sign changes from Eqs. 4–7 enables the removal of misalignment bias by appropriately defining an averaged friction coefficient as shown in Eq. 8.

$$\begin{aligned} \bar{\mu}' &= \frac{\frac{1}{2}(F_{Xf} - F_{Xr})}{F_{Y(\text{average})}} \\ \bar{\mu}' &= \frac{\mu F_n \cos(\alpha) - F_n \sin(\alpha) + \mu F_n \cos(\alpha) + F_n \sin(\alpha)}{F_n \cos(\alpha) + \mu F_n \sin(\alpha) + F_n \cos(\alpha) - \mu F_n \sin(\alpha)} \\ &= \frac{\mu F_n \cos(\alpha) + \mu F_n \cos(\alpha)}{F_n \cos(\alpha) + F_n \cos(\alpha)} = \frac{2\mu F_n \cos(\alpha)}{2F_n \cos(\alpha)} = \mu \end{aligned} \tag{8}$$

Averaging the forward and reverse forces and dividing appropriately provides an exact value of the interfacial friction coefficient for any combination of friction coefficient and misalignment angle. Thus, low and superlow friction coefficients can be accurately measured (within the measurement uncertainty) using this technique.

In many instruments, the vertical force is imposed using a dead weight load; the force is not measured and is assumed constant [3–9]. The reversal analysis is similar, but in this case $F_Y = mg$ remains constant. As the details in the Appendix demonstrate, the measured friction coefficient is given by Eq. 9.

$$\bar{\mu}' = \frac{\mu}{\cos(\alpha)^2 - \mu^2 \sin(\alpha)^2} \cong \mu \tag{9}$$

The biases do not vanish in this case, but they are reduced by orders of magnitude at low friction coefficients; for a friction coefficient of 0.01 and misalignment of 1°, the error using reversals is 0.01% vs. 280% without reversals. Reversals provide a robust route to substantially reduced misalignment bias for a variety of traditional tribometers.

It should be noted that the preceding X–Y analysis has neglected X–Z and Y–Z misalignments. These misalignments produce cosine errors in the friction force and normal force measurements, respectively. A Z-axis force measurement can be used to align the system if the needed degrees of freedom are available. If alignment is not possible, the Z-axis measurement can be used to account for the bias. It is difficult to determine the effects of the misalignments on the friction coefficient measurement without three orthogonal force measurements.

4 Measurement Uncertainty

The uncertainty analysis given here follows that of Schmitz et al. [1] and the ISO ‘‘Guide to the Expression of Uncertainty in Measurement’’ [2]. The uncertainties in individual measurements (forces) propagate into measurand (friction coefficient) calculations according to the Law

of Propagation of Uncertainty, as is shown mathematically in Eq. 10.

$$u_c(M)^2 = \sum_{i=1}^n \left(\frac{\partial M}{\partial x_i} \right)^2 u(x_i)^2 \quad (10)$$

Equation 8 is differentiated according to Eq. 10 to yield the square of the combined standard uncertainty of the averaged friction coefficient in terms of measurements and uncertainties in measurements as shown in Eq. 11,

$$\begin{aligned} u_c^2(\bar{\mu}') &= \left(\frac{1}{2F_{Y(\text{average})}} \right)^2 u^2(F_X) + \left(\frac{-1}{2F_{Y(\text{average})}} \right)^2 u^2(F_X) \\ &\quad + \left(\frac{-(F_{Xf} - F_{Xr})}{2F_{Y(\text{average})}^2} \right)^2 u^2(F_Y) \\ u_c^2(\bar{\mu}') &= \frac{1}{2} \left(\frac{1}{F_Y} \right)^2 u^2(F_X) + \left(\frac{F_X}{F_Y^2} \right)^2 u^2(F_Y) \end{aligned} \quad (11)$$

where F_X and F_Y are the average of absolute values and the average, respectively. This expression is simplified further with the use of a common force uncertainty and the definition of the averaged friction coefficient as shown by Eq. 12.

$$u_c^2(\bar{\mu}') = \frac{1}{2F_Y^2} (1 + 2\bar{\mu}'^2) \cdot u^2(F) \quad (12)$$

Taking the square root of Eq. 12 yields the combined standard uncertainty in the averaged friction coefficient which is largely just a function of F_Y and the force uncertainty.

$$u_c(\mu') = \frac{1}{\sqrt{2}F_Y} \sqrt{1 + 2\bar{\mu}'^2} u(F) \cong \frac{1}{\sqrt{2}F_Y} u(F) \quad (13)$$

5 Experimental Validation

The linear reciprocating tribometer shown in Fig. 3 was used to investigate the misalignment and reversal effects experimentally. The machining tolerances and the number of mated connections were minimized in an effort to minimize the resulting transducer misalignment. A control test performed without intentional misalignment gave friction coefficients of $\mu'_f = 0.1036 \pm 0.0016$ in the forward direction and $\mu'_r = 0.1045 \pm 0.0015$ in the reverse direction (taken from 1,000 measurements). Using these populations with Eqs. 4 and 7, the angular misalignment is calculated to lie in between 0.021° and 0.033° (~ 0.0005 mm/mm which indicates very tight tolerances) with 95% confidence.

The tribometer was also designed for small measurement uncertainties. A six-channel load cell is mounted directly to the sample, and unlike remote force sensing techniques with low friction gimbals, the load cell provides

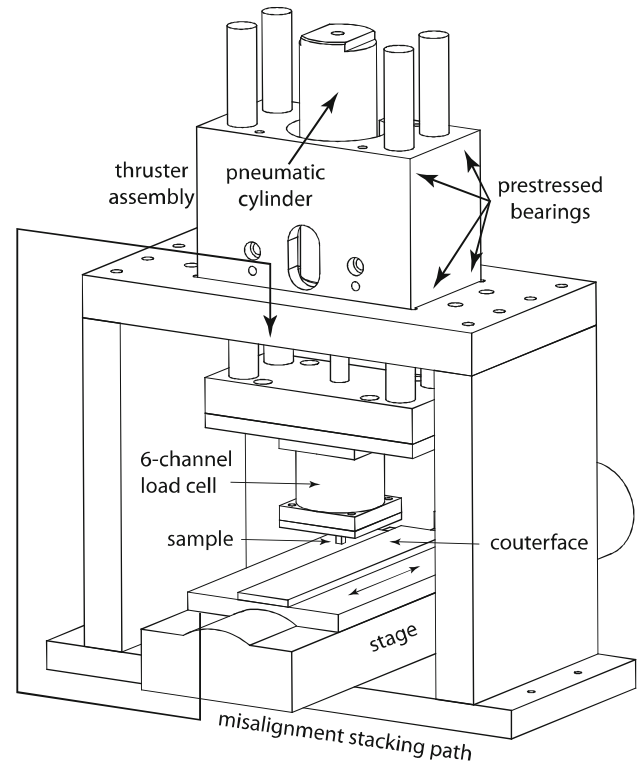


Fig. 3 Linear reciprocating tribometer used for experimental investigation of transducer misalignment and bias correction. The simple and symmetric design has a small number of mated surfaces to reduce the accumulation of angular misalignment between the transducer and counterface. The friction loop of the control experiment gives a misalignment of $\alpha = 0.027^\circ \pm 0.006^\circ$ which suggests that tight machining tolerances were held

the only force path to ground. In addition, measurements of normal force allow distinction between variations in friction coefficient and variations in normal force. The single component load cell makes the assumption of orthogonal axes reasonable. F_Y and F_X uncertainties were found (as described by Schmitz et al. [1] in detail) using mass standards and statistical methods to be approximately 0.7 N and 0.3 N, respectively. The uncertainty in the averaged friction coefficient was conservatively calculated using Eq. 13, a vertical force of 250 N and a common force uncertainty of 0.7 N, to be $u_c(\mu) = 0.002$.

For a controlled study of misalignment effects, measurements must be made at steady state and in the absence of wear with a single interfacial friction coefficient that is independent of track position and misalignment angle. These effects cannot be controlled; materials tend to stick at reversals, friction coefficients are sensitive to speed, position, transfer films, and wear; and varying misalignments can alter the area of contact. In an effort to minimize these effects, a 20 wt% PEEK/PTFE solid lubricant described in [10] was used for its unusual combination of wear resistance, uniform transfer films, and stable frictional

behavior. The pin has a nominal contact area of 6 mm × 6 mm and was tested under a 250 N normal load over a 25 mm stroke at 20 mm/s. Following a continuous 2 day run-in period, tests were conducted with various intentional misalignments. Feeler gages of 0.04 mm, 0.10 mm, 0.25 mm, 0.38 mm, 0.63 mm, and 1.25 mm thickness were used to elevate one side of a lapped 304 stainless steel counterface at a distance of 36.53 mm away from the contacting edge.

For each experiment, the forward and reverse F_Y and F_X forces were continuously measured and used to calculate forward and reverse friction coefficients continuously. These data are plotted versus the track position in Fig. 4. At zero misalignment, the friction loop appears visually centered about $\mu = 0$. As the misalignment angle increases, the friction loop tends downward. At 2°, the bias is nearly 50% of the interfacial friction coefficient.

The force data from each experiment were analyzed per Eq. 8 to obtain the interfacial friction coefficients as functions of wear track position. These ‘phase locked’ data are plotted versus track position in Fig. 5. Invariance of the results for varying misalignment gives an indication of the robustness of the method.

The data also contains rich information about the tribo-system. First, the interfacial friction coefficient does not decrease with increased misalignment due to the reduced ‘apparent contact area’ and increased pressure. Second, the frictional characteristics were incredibly stable from one experiment to the next despite unloading, shim insertion, and reloading. Third, it can be concluded that waviness

Fig. 4 Friction loops for varying angular misalignments between the transducer and the counterface. As the misalignment increases, the friction loop is further offset about zero. At 2°, the bias is about 50% of the friction coefficient

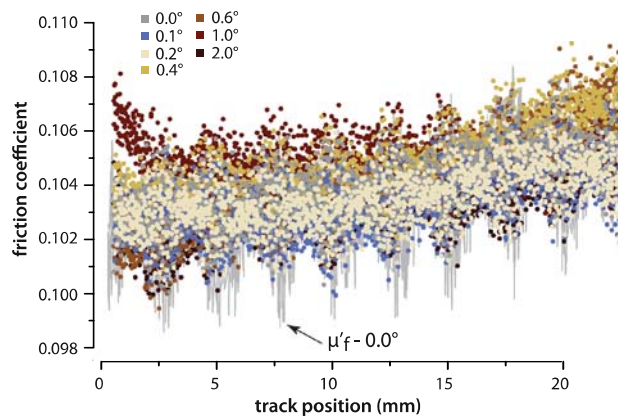
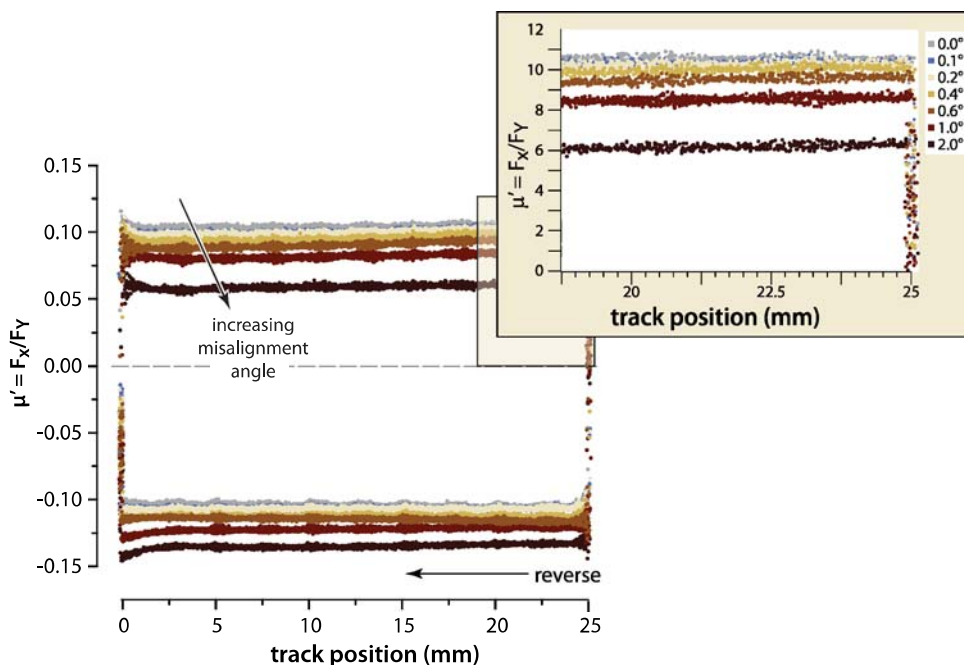


Fig. 5 Averaged friction coefficients plotted versus track position for various degrees of misalignment. The forward friction coefficient of the control experiment is shown as a gray line to demonstrate local variations and a general slope that are found only at high axis magnification. The recreation of these features following averaging indicates that these are systematic variations in the friction coefficient rather than random scatter. It also demonstrates the robustness of the technique and the stability of the interface with loading and unloading over the course of the experiment

effects are negligible. The forward friction coefficient at 0° misalignment is shown as a line plot behind the averaged friction coefficients in Fig. 5. Despite appearing very flat at the scale of Fig. 4, magnification in Fig. 5 reveals local fluctuations and a slight increase with increased sliding distance. With unidirectional data, these features might be mistakenly attributed to local waviness and counterface curvature, respectively. However, the reversal technique

eliminates these effects and indicates that the features reflect true variations in the friction coefficient. In addition, they are systematically reproduced at each misalignment condition, thus demonstrating a high degree of interfacial stability. The harmonics are likely artifacts from the stepper motor driven ball screw stage. The trend of increased friction coefficient with increased position is likely related to a variation in the transfer film that developed during the prior run-in period. As described in Burris and Sawyer [10], this particular composite material has extremely low wear rates in dry sliding conditions. Over the course of these experiments, it is unlikely that a single wear event occurred; it can be said with a high degree of confidence that this experiment was performed under wear-free interfacial sliding conditions.

The means and standard deviations of the forward, reverse, and averaged friction coefficients are given in Table 1 and plotted as functions of the misalignment angle in Fig. 6. At zero misalignment, the forward, reverse, and averaged data are essentially unaffected and accurately reflect the interfacial friction coefficient within the uncertainty in the measurement. Equations 4, 7, and 8 have been solved as functions of misalignment angle and are plotted as dashed lines in Fig. 6. The theoretical curves are bound by regions of 1 (containing 68% of the data) and 2 (containing 95% of the data) combined standard uncertainties to provide a visual envelope for the expected dispersion of measurement values. The averaged, forward, and reverse friction coefficients are within the bounds of expected behavior. For seven experiments with widely varying misalignment angles, the measured friction coefficients are in excellent agreement giving a mean friction coefficient of $\mu = 0.1040$ and a standard deviation of $\sigma = 0.0006$.

Table 1 Means and standard deviations from 1,000 measurements of forward (μ_f), reverse (μ_r) and averaged friction coefficient for varying misalignments

α (°)	μ'_f	$\sigma(\mu'_f)$	μ'_r	$\sigma(\mu'_r)$	μ	$\sigma(\mu)$
0.000	0.1036	0.0016	0.1045	0.0015	0.1039	0.0012
0.060	0.0998	0.0020	0.1064	0.0011	0.1034	0.0012
0.160	0.0997	0.0021	0.1068	0.0011	0.1035	0.0011
0.399	0.0956	0.0029	0.1121	0.0011	0.1047	0.0014
0.598	0.0905	0.0027	0.1143	0.0013	0.1042	0.0018
0.996	0.0816	0.0029	0.1219	0.0011	0.1050	0.0008
1.992	0.0566	0.0021	0.1364	0.0014	0.1034	0.0012
Average					0.1040	
SD					0.0006	

The averaged friction coefficient is mathematically identical to the interfacial friction coefficient, μ . The reversal technique provides a robust friction coefficient measurement independent of the transducer misalignment angle

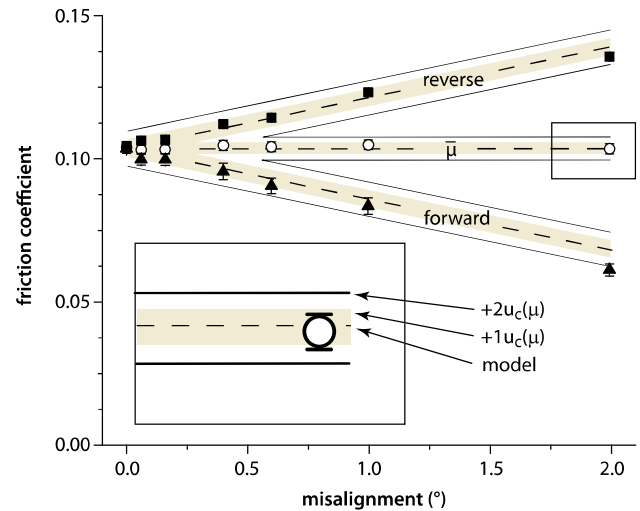


Fig. 6 Friction coefficient measurements plotted versus misalignment angle. Calculations of the expected behaviors plus and minus one and two standard uncertainties are also plotted. The data lie within the envelope of expected behavior and the interfacial friction coefficient is accurately measured at all misalignment angles

6 Conclusions

- 1) A simple analysis of the angular misalignment between the counterface and transducer indicates that friction coefficient measurements are extremely sensitive to misalignments from realistic manufacturing tolerances.
- 2) A reversal technique has been proposed as a simple and robust means to eliminate misalignment induced biases in friction coefficient measurements.
- 3) Results of experiments with controlled misalignment angles reflected the predicted sensitivity. A model low wear interface was used to demonstrate that the reversal technique completely eliminated the misalignment sensitivity and revealed rich details in the frictional characteristics that could not otherwise be discerned from waviness.

Acknowledgments Financial support for this work was provided through an AFOSR-MURI grant FA9550-04-1-0367. We would also like to thank Prof. T. L. Schmitz and Prof. J. C. Ziegert for many helpful discussions regarding tribometry and uncertainty analysis.

Appendix

Analysis of Dead-Weight Loading

Most tribometers avoid measurements of normal force by prescribing it with a dead-weight. F_Y is constant and equal to the product of mass and the gravitation acceleration

(mg). In this case, the normal force changes when the motion path reverses. Using mg for F_Y in Eq. 3 gives,

$$F_{nf} = \frac{mg}{\cos(\alpha) - \mu \sin(\alpha)} \quad (14)$$

Similarly for Eq. 6,

$$F_{nr} = \frac{mg}{\cos(\alpha) - \mu \sin(\alpha)} \quad (15)$$

Using these definitions in Eqs. 2 and 5 gives,

$$F_{Xf} = \frac{mg \cdot \mu \cos(\alpha)}{\cos(\alpha) + \mu \sin(\alpha)} - \frac{mg \cdot \sin(\alpha)}{\cos(\alpha) + \mu \sin(\alpha)} \quad (16)$$

$$F_{Xr} = \frac{-mg \cdot \mu \cos(\alpha)}{\cos(\alpha) - \mu \sin(\alpha)} - \frac{mg \cdot \sin(\alpha)}{\cos(\alpha) - \mu \sin(\alpha)} \quad (17)$$

Inserting Eqs. 16 and 17 into Eq. 8 gives the averaged friction coefficient,

$$\begin{aligned} \bar{\mu}' &= \frac{\frac{1}{2}(F_{Xf} - F_{Xr})}{F_{Y(\text{average})}} = \frac{F_{Xf} - F_{Xr}}{2 \cdot mg} \\ &= \frac{\frac{mg \cdot \mu \cos(\alpha)}{\cos(\alpha) + \mu \sin(\alpha)} - \frac{mg \cdot \sin(\alpha)}{\cos(\alpha) + \mu \sin(\alpha)} + \frac{mg \cdot \mu \cos(\alpha)}{\cos(\alpha) - \mu \sin(\alpha)} + \frac{mg \cdot \sin(\alpha)}{\cos(\alpha) - \mu \sin(\alpha)}}{2 \cdot mg} \\ &= \frac{\mu}{\cos(\alpha)^2 - \mu^2 \sin(\alpha)^2} \cong \mu \end{aligned} \quad (18)$$

References

- Schmitz, T., Action, J., Ziegert, J., Sawyer, W.: The difficulty of measuring low friction: uncertainty analysis for friction coefficient measurements. *J. Tribol. Trans. ASME* **127**, 673–678 (2005). doi:[10.1115/1.1843853](https://doi.org/10.1115/1.1843853)
- International Standards Organization (ISO): Guide to the expression of uncertainty in measurement (1993, Corrected and Reprinted 1995)
- McCook, N., Burris, D., Bourne, G., Steffens, J., Hanrahan, J., Sawyer, W.: Wear resistant solid lubricant coating made from PTFE and epoxy. *Tribol. Lett.* **18**, 119–124 (2005). doi:[10.1007/s11249-004-1766-7](https://doi.org/10.1007/s11249-004-1766-7)
- Blanchet, T., Kennedy, F.: Sliding wear mechanism of polytetrafluoroethylene (PTFE) and PTFE composites. *Wear* **153**, 229–243 (1992). doi:[10.1016/0043-1648\(92\)90271-9](https://doi.org/10.1016/0043-1648(92)90271-9)
- Flom, D., Porile, N.: Friction of teflon sliding on teflon. *J. Appl. Phys.* **26**, 1088–1092 (1955). doi:[10.1063/1.1722156](https://doi.org/10.1063/1.1722156)
- Makinson, K., Tabor, D.: Friction + transfer of polytetrafluoroethylene. *Nature* **201**, 464–476 (1964). doi:[10.1038/201464a0](https://doi.org/10.1038/201464a0)
- McLaren, K., Tabor, D.: Visco-elastic properties and friction of solids—friction of polymers—influence of speed and temperature. *Nature* **197**, 856–858 (1963). doi:[10.1038/197856a0](https://doi.org/10.1038/197856a0)
- Steijn, R.: Sliding experiments with polytetrafluoroethylene. *ASLE Trans.* **11**, 235–245 (1968)
- Tanaka, K., Uchiyama, Y., Toyooka, S.: Mechanism of wear of polytetrafluoroethylene. *Wear* **23**, 153–172 (1973). doi:[10.1016/0043-1648\(73\)90081-1](https://doi.org/10.1016/0043-1648(73)90081-1)
- Burris, D., Sawyer, W.: A low friction and ultra low wear rate PEEK/PTFE composite. *Wear* **261**, 410–418 (2006). doi:[10.1016/j.wear.2005.12.016](https://doi.org/10.1016/j.wear.2005.12.016)